Bioorganic & Medicinal Chemistry Letters 23 (2013) 673–678

Contents lists available at SciVerse ScienceDirect

Bioorganic & Medicinal Chemistry Letters

journal homepage: www.elsevier.com/locate/bmcl

Lead optimization of a dihydropyrrolopyrimidine inhibitor against phosphoinositide 3-kinase (PI3K) to improve the phenol glucuronic acid conjugation

Hatsuo Kawada [a,*], Hirosato Ebiike [b], Masao Tsukazaki [b], Mitsuaki Nakamura [b], Kenji Morikami [a], Kiyoshi Yoshinari [b], Miyuki Yoshida [b], Kotaro Ogawa [a], Nobuo Shimma [b], Takuo Tsukuda [b], Jun Ohwada [b]

[a] Research Division, Chugai Pharmaceutical Co., Ltd, 1-135 Komakado, Gotemba, Shizuoka 412-8513, Japan
[b] Research Division, Chugai Pharmaceutical Co., Ltd, 200 Kajiwara, Kamakura, Kanagawa 247-8530, Japan

ARTICLE INFO

Article history:
Received 14 September 2012
Revised 22 November 2012
Accepted 27 November 2012
Available online 3 December 2012

Keywords:
PI3K
Cancer
SBDD
Bioisostere
Glucuronic acid conjugation

ABSTRACT

Our lead compound for a phosphoinositide 3-kinase (PI3K) inhibitor (**1**) was metabolically unstable because of rapid glucuronidation of the phenol moiety. Based on structure–activity relationship (SAR) information and a FlexSIS docking simulation score, aminopyrimidine was identified as a bioisostere of phenol. An X-ray structure study revealed a hydrogen bonding pattern of aminopyrimidine derivatives. Finally, aminopyrimidine derivatives **33** showed strong tumor growth inhibition against a KPL-4 breast cancer xenograft model in vivo.

Phosphoinositide 3-kinase (PI3K) pathway is activated in various human cancers and have recently been ~ target.[1,2] Among the three PI3K family members (class I, II, III), class I PI3Ks are a well-known promising target for cancer treatment because, by converting phosphatidylinositol-4,5-bisphosphate (PI(4,5)P2) to phosphatidylinositol-3,4,5-triphosphate (PI(3,4,5)P3) which then activates the protein serine/threonine kinase AKT, they regulate a range of cellular functions including cell cycle and cell survival promotion.[3] In addition, although PI(3,4,5)P3 is converted back to PI(4,5)P2 by tumor suppressor PTEN, loss of heterozygosity and mutations of PTEN are observed in various human cancers.[4] Class I PI3Ks are heterodimers consisting of a p110 catalytic subunit and a p85 regulatory subunit. Of four known p110 isoforms (α, β, γ, and, δ), significant efforts have focused on developing a p110α (PI3Kα) inhibitor because frequent oncogenic mutations and gene amplifications of p110α are found in human cancers.[1,5,6]

In this Letter, we describe details of optimizing our lead dihydropyrrolopyrimidine PI3K inhibitor to overcome the issue of rapid glucuronidation of the phenol moiety. Our approaches to solving the issue were bioisosteric modifications and molecular design of the phenol part using a virtual docking study. In addition, we report details, based on the X-ray study, of the interactions between PI3K protein and our dihydropyrrolopyrimidine inhibitor with aminopyrimidine moiety.

As we have already reported,[7] we designed and identified the dihydropyrrolopyrimidine PI3K inhibitor **1** as a lead compound by superimposing PIramed's PI103 (**2**)[8] and Chiron's PI3K inhibitor (**3**)[9] based on their docking models against the crystallographic structure of PI3K (Fig. 1) and found that compound **1** inhibited PI3Kα with IC_{50} value of 0.0086 μM.[10]

First, we modified the 4-pyridyl moiety of compound **1**. Because the modeling suggested 4-pyridyl moiety extends to the solvent-exposed region of PI3K and no clear interaction between 4-pyridyl moiety and PI3K was specified, various kinds of heteroaromatic ring were introduced. As shown in Table 1, removal of the nitrogen atom significantly decreased activity (**6**) and several heteroaromatic rings, such as benzoimidazole (**10**) or thiazole (**11**), showed moderate inhibitory activity but the most potent substituent was pyridine. In the case of pyridine, the position of the nitrogen atom was critical and 4-pyridyl was the best among three pyridine regioisomers (**1**, **4**, **5**).

Unfortunately, oral bioavailability of compound **1** in mouse was extremely low (1.6%). Further investigation suggested **1** is rapidly metabolized by glucuronidation of phenol and the $T_{1/2}$ in an in vitro glucuronidation study was 11 min in human and 6.1 min

* Corresponding author. Tel.: +81 0550 87 8364; fax: +81 0550 87 5326.
E-mail address: kawadahto@chugai-pharm.co.jp (H. Kawada).

0960-894X/$ - see front matter © 2012 Elsevier Ltd. All rights reserved.
http://dx.doi.org/10.1016/j.bmcl.2012.11.112

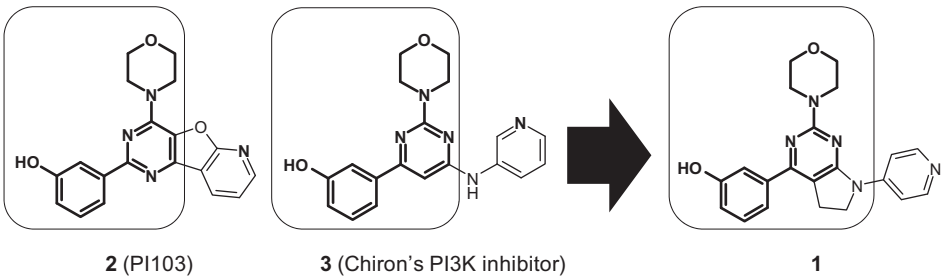

Figure 1. Lead generation.

Table 1
In vitro activity of heteroaromatic compounds

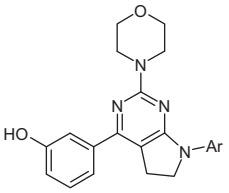

Compound	Ar	PI3Kα IC_{50} (μM)
1		0.0086
4		0.041
5		>50
6		1.22
7	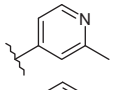	0.17
8	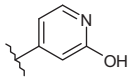	0.20
9	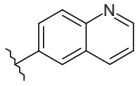	>50
10	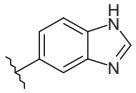	0.077
11		0.049
12	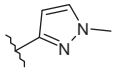	0.23

Table 2
In vitro activity of phenol derivatives

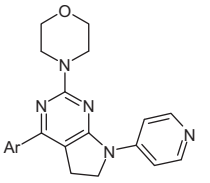

Compound	Ar	PI3Kα IC_{50} (μM)
13	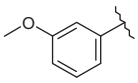	0.41
14	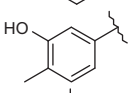	>50
15	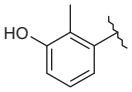	>50

in mouse.[11] To avoid this rapid metabolism, phenol was protected as methyl ether (**13**) but the activity was 50-fold lower than **1** (Table 2). Introducing an ortho methyl group to block glucuronidation also lost activity (**14**, **15**). Based on the X-ray crystal structure of **10** in PI3Kγ (Fig. 2), various phenol bioisosteres that have a hydrogen bond donor and acceptor were evaluated (**16**–**20**) but their inhibitory activity was weak (Table 3).

The heteroaromatic ring was also tested (Table 4). Although indazole derivatives lost inhibitory activity, benzoimidazole (**21**) showed moderate activity. As shown in Table 5, further investigation of the heteroaromatic ring revealed a clear SAR of pyridine derivatives. 3-Pyridyl derivative (**28**) was 10 times more potent than 4-pyridyl (**27**) and 3,5-pyrimidyl (**29**) was much stronger again. In addition, a FlexSIS docking simulation[12] of virtual compounds with PI3Kγ that was based on the X-ray structure information of PI3Kγ with compound **10** gave a good score for aminopyridyl derivatives, such as 4-amino-2-pyridyl (**30**), 4-amino-3-pyridyl (**31**) and 4-amino-3,5-pyrimidyl (**32**). FlexSIS scores of **30**, **31** and **32** were −27.3, −25.8 and −25.5 kJ/mol, respectively, all lower than that of **10** (−23.3 kJ/mol). As shown in Table 6, these compounds showed good inhibitory activity against PI3Kα and 4-amino-3,5-pyrimidyl was the most potent, with an IC_{50} value of 0.026 μM (**32**).

The strong potency of 4-amino-3,5-pyrimidyl derivatives was confirmed by an X-ray structure analysis of compound **33** with PI3Kγ (Fig. 2).[13] In the case of the hydrogen bonding pattern of compound **10**, the hydroxyl group of phenol interacts with Asp841 and Tyr867. In the case of compound **33**, the amino group of aminopyrimidine is located between Asp836 and Asp841 and makes a hydrogen bond with Asp836 (the distance between the nitrogen of the amino group and the oxygen of Asp836 is 3.0 Å) and an attractive electrostatic interaction with Asp841 (distance between the nitrogen of the amino group and the oxygen of Asp841 is 3.7 Å, which is not close enough for a hydrogen bond to form). In addition, one of the nitrogen atoms of the pyrimidine ring interacts with the side chain NH_3^+ of Lys833, and the other nitrogen makes a weak attractive electrostatic interaction with OH of Tyr867 (distance between the oxygen of Tyr867 and the nitrogen of pyrimidine of **33** is 4.3 Å, which is not close enough for a hydrogen bond). Notably, in order to make these hydrogen bonds possible, the dihydropyrrolopyrimidine core structure of

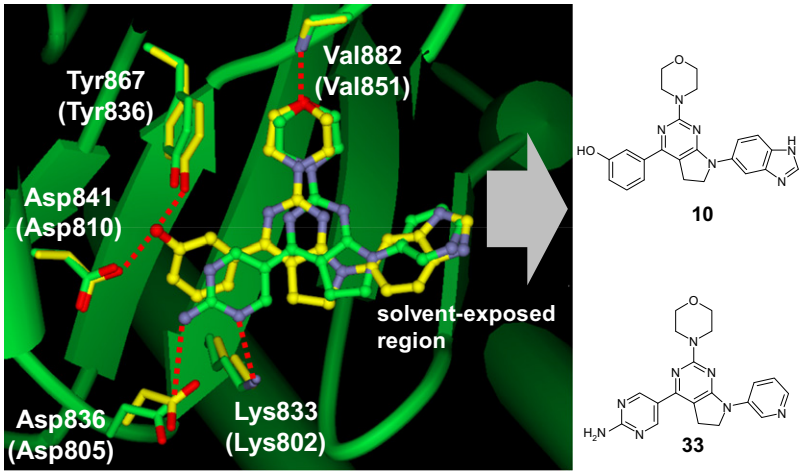

Figure 2. Crystal structure of **10** (shown in yellow) and **33** (shown in green) in PI3Kγ. Numbering of PI3Kα is shown in parentheses.

Table 3
In vitro activity of phenol bioisosteres

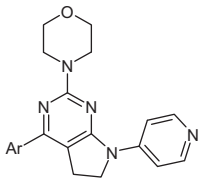

Compound	Ar	PI3Kα IC_{50} (μM)
16	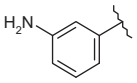	3.7
17	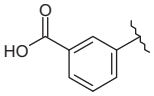	>50
18	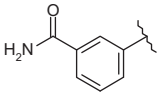	19
19	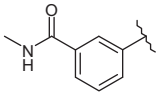	2.4
20	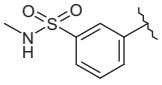	>50

Table 4
In vitro activity of benzoimidazole and indazoles

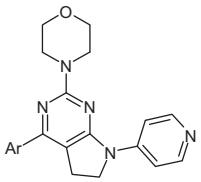

Compound	Ar	PI3Kα IC_{50} (μM)
21	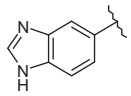	0.30
22	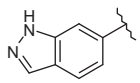	>50
23	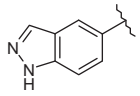	>50
24	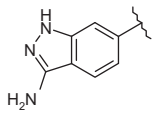	>50
25	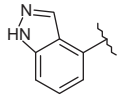	>50
26	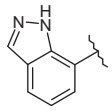	>50

33 shifted closer toward the solvent-exposed region than that of the phenol compound **10**.

As shown in Table 7,[14,15] compound **32** and **33** showed strong in vitro anti-proliferative activity against human cancer cell lines that are known as PI3Kα mutant or PTEN null. The $T_{1/2}$ of these compounds in in vitro glucuronidation was over 60 min both in human and mouse. Compound **33** showed remarkably improved bioavailability (41%) in mice compared to lead compound **1** (Table 8).[16] As presented in Figure 3, compound **33** showed strong tumor growth inhibition (166%) against the KPL-4[17] human breast cancer cell line (PI3Kα H1047R mutant) at a dose of 80 mg/kg.[18]

Synthetic routes of our PI3K inhibitors are summarized in Scheme 1. Compound **36** was identified as a key intermediate for optimizing the substituent at the solvent-exposed region and various aniline derivatives were coupled with **36** (Route A: applied for compound **1**, **4**, **5**, **7**–**13**). To optimize the aryl group of phenol position, we first introduced various aryl groups for γ-butyrolactone **34** (Route B: applied for compound **14**, **15**, **20**, **28**), and later applied Suzuki coupling[19] to useful key intermediate **43** (Route C: applied for compound **6**, **16**–**19**, **21**–**27**, **29**–**33**). Representative experimental procedures are available in the Supplementary data.

In summary, based on SARs and a FlexSIS docking simulation, 4-amino-3,5-pyrimidyl derivative was identified as a bioisostere of metabolically unstable 3-hydroxyphenyl derivative. 4-amino-3,5-pyrimidyl derivatives **32** and **33** showed comparable PI3K inhibitory activity to **1** and greatly improved metabolic stability. X-ray structure analysis of PI3Kγ with **33** revealed the newly-formed

Table 5
In vitro activity of pyridine derivatives

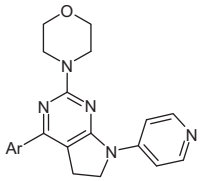

Compound	Ar	PI3Kα IC_{50} (μM)
27		22.6
28		1.70
29		0.44

Table 6
In vitro activity of aminopyridine derivatives

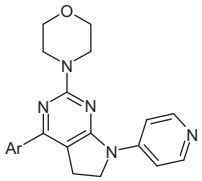

Compound	Ar	PI3Kα IC_{50} (μM)
30	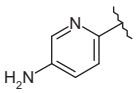	0.34
31	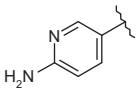	0.24
32	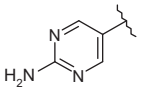	0.026

Table 7
Improvement of glucuronidation and liver microsome (LM) stability

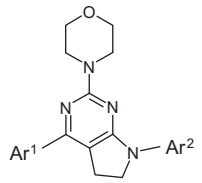

Compound	Ar^1	Ar^2	IC_{50} (μM)				Glucuronidation $T_{1/2}$ (min)		LM stablility $T_{1/2}$ (min)	
			PI3Kα	HCT116[a]	PC-3[b]	KPL-4[c]	Human	Mouse	Human	Mouse
1	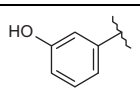		0.0086	0.72	0.14	0.45	11	6.1	21	20
32	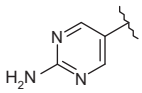		0.026	0.091	0.12	0.029	>60	>60	127	27
33	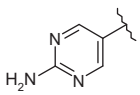		0.033	0.17	0.42	0.015	>60	>60	71	63

[a] CRC, PI3Kα H1047R.
[b] Prostate cancer, PTEN negative.
[c] Breast cancer, PI3Kα H1047R.

Table 8
Mouse PK profile of **33**

Mouse PK (10 mg/kg iv)			Mouse PK (100 mg/kg po)				
AUC (ng/mL h)	CL (mL/min/kg)	$T_{1/2}$ (h)	C_{max} (ng/mL)	AUC (ng/mL h)	CL/F (mL/min/kg)	$T_{1/2}$ (h)	F (%)
4690	35.9	10.3	4190	19400	86.1	6.58	41

Pharmacokinetic parameters of **33** in female nude mice following an intravenous (10 mg/kg) and an oral (100 mg/kg) administration of **33**. Values represent the mean of two animals.

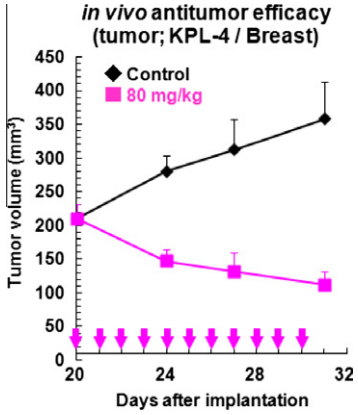

Figure 3. In vivo antitumor activity of **33** in the KPL-4 mouse xenograft model. KPL-4 cells were orthotopically injected into female BALB-nu/nu mice (Charles River Laboratories Japan). The compound was orally administered once daily.

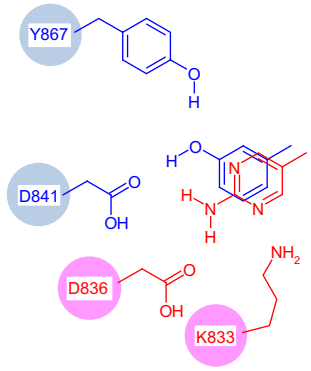

Figure 4. Interactions of phenol of **10** and aminopyrimidine of **33**.

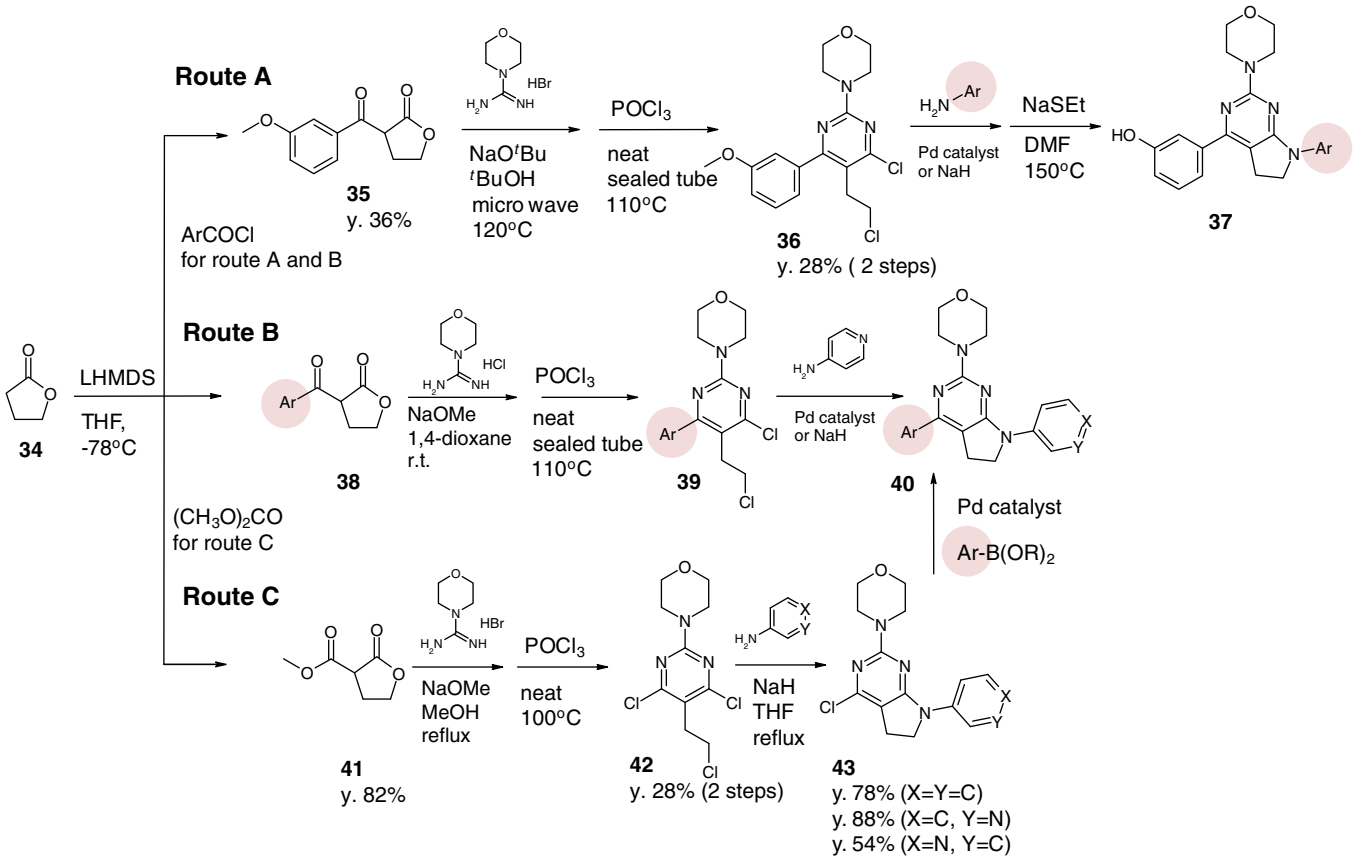

Scheme 1. Alternative synthetic routes for lead optimization.

hydrogen bonds with Asp836 and Lys833 and the slight shift of the whole inhibitor toward the solvent-exposed region. When modifying the phenol moiety, we first concentrated on the interactions with Asp841 and Tyr867 (depicted in blue in Fig. 4) based on the X-ray structure of **10**, but the results of this approach were not successful. The virtual docking of the whole active site took into consideration not only Asp841 and Tyr867, but also Asp836 and Lys833 (depicted in red in Fig. 4). Considering the whole active site by virtual docking in this way resulted in finding the 4-amino-3,5-pyrimidyl derivative, which has interactions not only between Asp841 and Tyr867 (a weak electrostatic interaction) but also between Asp836 and Lys833 (a strong hydrogen bond). Finally, aminopyrimidine derivative **33** showed strong tumor growth inhibition in a KPL-4 xenograft model in mouse.

Acknowledgments

We thank H. Suda for glucuronidation assays. We thank T. Fujii and K. Sakata for biological assays. We thank S. Kuramoto for PK studies. We thank S. Courtney and W. Trigg (Evotec) for synthetic assistance. We thank the staffs of synchrotron beam lines NW12 at PF, and of KEK and BL41XU at SPring-8 for their help in data collection. We are grateful to Dr. Junichi Kurebayashi for providing KPL-4 cells.

Supplementary data

Supplementary data associated with this article can be found, in the online version, at http://dx.doi.org/10.1016/j.bmcl.2012.11.112. These data include MOL files and InChiKeys of the most important compounds described in this article.

References and notes

1. Liu, P.; Cheng, H.; Roberts, T. M.; Zhao, J. J. *Nat. Rev. Drug Disc.* **2009**, *8*, 627.
2. Engelman, J. A.; Luo, J.; Cantley, L. C. *Nat. Rev. Genet.* **2006**, *7*, 606.
3. Cantley, L. C. *Science* **2002**, *296*, 1655.
4. Vivanco, I.; Sawyers, C. L. *Nat. Rev. Cancer* **2002**, *2*, 489.
5. Parsons, D. W.; Wang, T. L.; Samuels, Y.; Bardelli, A.; Cummins, J. M.; DeLong, L.; Silliman, N.; Ptak, J.; Szabo, S.; Willson, J. K.; Markowitz, S.; Kinzler, K. W.; Vogelstein, B.; Lengauer, C.; Velculescu, V. E. *Nature* **2005**, *436*, 792.
6. Samuels, Y.; Wang, Z.; Bardelli, A.; Silliman, N.; Ptak, J.; Szabo, S.; Yan, H.; Gazdar, A.; Powell, S. M.; Riggins, G. J.; Willson, J. K.; Markowitz, S.; Kinzler, K. W.; Vogelstein, B.; Velculescu, V. E. *Science* **2004**, *304*, 554.
7. Ohwada, J.; Ebiike, H.; Kawada, H.; Tsukazaki, M.; Nakamura, M.; Miyazaki, T.; Morikami, K.; Yoshinari, K.; Yoshida, M.; Kondoh, O.; Kuramoto, S.; Ogawa, K.; Aoki, Y.; Shimma, N. *Bioorg. Med. Chem. Lett.* **2011**, *21*, 1767.
8. Hayakawa, M.; Kaizawa, H.; Moritomo, H.; Kawaguchi, K.; Koizumi, T.; Yamano, M.; Matsuda, K.; Okada, M.; Ohta, M.; WO Patent, 1083456, 2001.
9. Nuss, J M.; Pecchi, S.; Renhowe, P A.; WO Patent, 4048365, 2004.
10. *Kinase assay:* The inhibitory activity on PI3Kα (p110α/p85α) (Life Technologies) was determined by Adapta Universal Kinase Assay Kit with PIP2:PS Lipid Kinase Substrate (Life Technologies).
11. *UGT–glucuronidation activity assay:* Human (or Mouse) liver microsome (1.0 mg protein/ml) was incubated in 50 mM Tris–HCl (pH 7.5) buffer containing 25 μg/ml alamethicin at 4 °C for 30 min. Then, the UDP-glucuronosyltransferases were released from the inside of the endoplasmic reticulum membranes. Five micromolar of each compound was incubated in human (or mouse) liver microsome solution with 2 mM of UDPGA (UDP–glucuronic acid) cofactor at 37 °C for 60 min. After the enzyme reaction was terminated with the addition of a threefold volume of acetonitrile, the reaction mixture was centrifuged at 1500 rpm for 10 min. The resultant supernatant was used as a test sample to measure the glucuronidation activity catalyzed by human (or mouse) microsome by quantitating the compound in the sample using LC/MS/MS.
12. Rarey, M.; Kramer, B.; Lengauer, T.; Klebe, G. *J. Mol. Biol.* **1996**, *261*, 470. Compounds were docked to the crystal structure of PI3Kγ complexed with **10** (PDB: 3APF) by the in silico docking tool, FlexSIS, while the dihydropyrrolopyrimidine moiety was fixed to the position of compound **10** in the crystal structure. Docking scores were defined by the FlexSIS standard scoring.
13. PDB ID code: 3APD.
14. *Cell proliferation assay:* The breast cancer KPL-4, colon cancer HCT116 (ATCC) and prostate cancer PC-3 (ATCC) cells were treated with various concentrations of assay compounds for 96 h. Cell growth inhibition was determined by Cell Counting Kit-8 solution (Dojindo Laboratories).
15. *Microsomal stability* assay: One micromolar of each compound was incubated with human (or mouse) liver microsome (0.5 mg protein/ml) in 50 mM phosphate buffer (pH 7.4) containing 1 mM NADPH (the reduced form of nicotinamide adenine dinucleotide phosphate) at 37 °C for 30 min. After the enzyme reaction was terminated with the addition of a threefold volume of acetonitrile, the reaction mixture was centrifuged at 1500 rpm for 10 min. The resultant supernatant was used as a test sample to measure the stability in human (or mouse) liver microsome by quantitating the compound in the sample using LC/MS.
16. *Pharmacokinetic study:* Female BALB/c-nu mice ($n = 2$ per treatment group) were given 33 by intravenous (iv) or oral (po) route at doses of 10 and 100 mg/kg, respectively. Blood samples of each animal were collected with heparin as an anticoagulant at 0.08, 0.25, 2, 4, 7, and 24 h following iv dosing and at 0.50, 2, 4, 7, and 24 h following po dosing. Samples were centrifuged to obtain plasma and stored at −80 °C until analysis. Plasma concentrations were determined by using LC–MS/MS system. The pharmacokinetic parameters were calculated by non-compartmental analysis using WATSON ver. 7.1 (Thermo Fisher Scientific, Wayne, PA).
17. Kurebayashi, J.; Otsuki, T.; Tang, C. K.; Kurosumi, M.; Yamamoto, S.; Tanaka, K.; Mochizuki, M.; Nakamura, H.; Sonoo, H. *Br. J. Cancer* **1999**, *79*, 707.
18. *In vivo study:* KPL-4 cells were orthotopically injected into the mammary fat pad of female BALB-nu/nu mice (Charles River Laboratories Japan). Tumor size was measured using a gauge twice per week, and tumor volume (TV) was calculated using the following formula: $TV = ab^2/2$, where a is the length of the tumor, and b is the width. Once the tumors reached a volume of approximately 200 mm^3, animals were randomized into groups ($n = 5$ in each group), and treatment was initiated. The compound was orally administered once daily for 11 days.
19. Miyaura, N.; Suzuki, A. *Chem. Rev.* **1995**, *95*, 2457.